Fast MTF and Aberrations Analysis of MWIR and LWIR Imaging Systems using Quadri Wave Interferometry

Sabrina Velghe[1], Emeline Durand, Djamel Brahmi, William Boucher, Benoit Wattellier
PHASICS S.A., Campus de l'Ecole Polytechnique, Palaiseau 91128, France.

ABSTRACT

We present the application of Quadri-Wave Lateral Shearing Interferometry (QWLSI), a wave front sensing technique, to characterize optical beams at infrared wavelengths from 2 to 16µm with a single instrument. We apply this technique to qualify optical systems dedicated to MWIR (λ within 3 and 5µm) and LWIR (λ within 8 and 14µm) wavelength ranges. The QWLSI offers the crucial advantage that it yields an analyzed wave front without the use of a reference arm and consequent time consuming alignment. The qualification of an optical system with QWLSI gives a complete diagnostic, from the aberration cartography to the PSF and MTF curves for every direction in one single measurement. In this paper, we first present the QWLSI technology and its main features, we also detail an experimental comparison between our MTF measurement and the results given by a classical MTF test bench. We finally show the experimental analysis of an infrared lens at two different wavelengths, one in the MWIR range (λ=3.39µm) and the other in the LWIR range (λ=10.6µm).

Keywords: Infrared, Thermal Imaging, Optical Metrology, Wave Front Sensing, Aberration, PSF, MTF.

1. INTRODUCTION

In the last years, infrared imagery has known a rapid expansion due to its large applications (intelligence gathering, security issue, night vision, thermography, …). This expansion has been accompanied by the progress of infrared detectors' technology allowing the production of large scale detector array (320x256, 640x512 pixels). The increasing demand of high-performance systems is supported by the need of control systems with high sensitivity, particularly concerning the qualification of their optical parts.

Though MTF remains the first standard objective qualification, it does not diagnose possible defects of the analyzed objective (misalignment of lenses, inadequate aspherization,…). For the qualification of infrared objectives, current techniques based on interferometric set-up are complex and the alignment procedure for the analysis of one objective is time consuming. For these practical reasons, most of the objectives are simply tested on MTF benches. We propose to use a wave front sensor that directly analyzes the light transmitted by an objective and gives its aberrations. Therefore, this considerably simplifies the qualification process. The Quadri-Wave Lateral Shearing Interferometry is a good answer to infrared optical metrology due to its metrological qualities (high resolution, high precision and dynamic) and offers cost-effective solutions.

2. QWLSI TECHNOLOGY

2.1 QWLSI origins

Our technology is based on Quadri Wave Lateral Shearing Interferometry, invented by Jerôme Primot [1] at Onera. It uses a 2D diffraction grating called "Modified Hartmann Mask" (MHM). It takes its origin in the classical Hartmann test using a mask made of square holes. In 1971, Shack proposed an evolution of this solution by replacing the mask by a micro-lens array [2], and by this way creating the well-known Shack-Hartmann wave front sensors. In the 90's, facing

[1] info@phasics.fr ; phone +33 (0)1 69 33 89 99 ; fax +33 (0)1 69 33 89 88 ; www.phasics.com

high resolution needs, Jerôme Primot suggested to come back to the Hartmann test while adding a π-shift phase checker board [1] (see Figure 1).

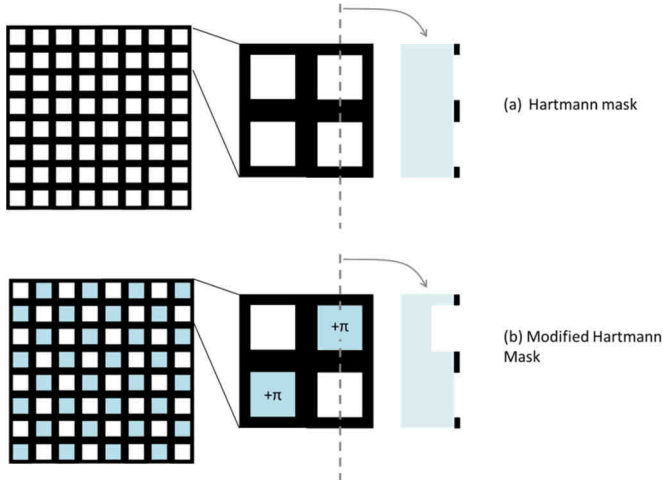

Figure 1 Differences between a Hartmann Mask (a) and a Modified Hartmann Mask (b). The Hartmann mask is here obtained by metal deposition (black straits) on an optical substrate, the MHM is completed by adding a phase checker board (obtained by etching process).

The basic idea of many wave front sensors derived from the Harmtann test is to create an intensity modulation and to analyze its deformation when illuminated by an aberrated wave front. This deformation is directly related to wave front gradients in both x- and y-directions. From the gradients, the original wave front is recovered by numerical integration [3].

2.2 High dynamic range with high accuracy

With the micro-lens array or the Hartmann mask, the modulation pattern contrast, and thus the measurement signal-to-noise ratio, depends on the CCD position and on the aberrations themselves. In some circumstances, the modulation vanishes and no measurement is possible. Adding the π-shift phase checker board to the Hartmann mask overcomes this limitation. This implies high accuracy even for large aberrations.
To show this, we plot on Figure 2, the evolution of the intensity profile going through one lens (a), a Hartmann test (b) and a MHM (c) along the propagation axis z.

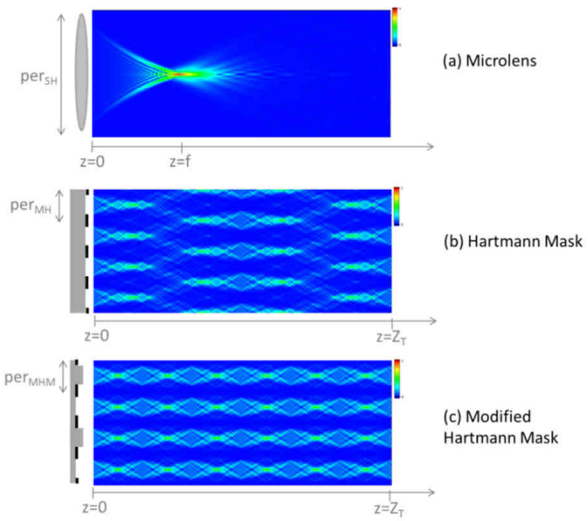

Figure 2 Evolution of the intensity profile according the propagation axis z through a lens, a Hartmann mask and a Modified Hartmann Mask

For the lens case, the beam simply converges to the focal spot and then diverges. The intensity modulation has a high contrast only at the vicinity of the focal spot. The behavior of the Hartmann mask is more complicated due to diffraction effects. The contrast depends on the observation plane: at some planes, the intensity is focused and a few mm further it becomes almost uniform (the measure is difficult at those planes). Nevertheless, the so-called "Talbot effect" states that the Hartmanngram contrast is periodic with the distance from mask to CCD: the period is equal to the Talbot distance Z_T [4]. For a plane wave, Z_T is equal to $2per_{MH}^2/\lambda$ (where per_{MH} is the spatial period of the Hartmann mask and λ the wavelength). If the beam is diverging or converging, Z_T is altered and depends on the numerical aperture of the impinging beam: the Talbot planes become closer when the beam is converging and move away when it is diverging [5]. Thus for a diverging or converging beam, the modulation contrast changes with the magnitude of aberration: it is therefore difficult to predict the measurement accuracy for large aberrations.

For the MHM, due to the π-shift phase checker board, the 0th-diffraction order vanishes. This implies that the Talbot distance vanishes also. Consequently the Hartmanngram contrast becomes independent of the distance from the mask to CCD and the measurement accuracy is kept whatever the aberration dynamic range. This property can be used to measure high numerical aperture beam as schematically shown on Figure 3 (up to F/1 with our infrared sensor) and beams with high dynamic aberrations.

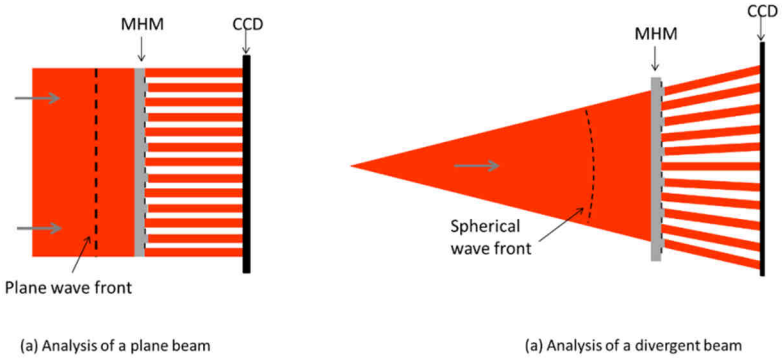

Figure 3 Principle of the analysis of a plane beam (a) and a divergent beam (b) with a MHM

2.3 High resolution wave front sensing

As the diffracted orders of a MHM are mainly constituted of the ±1 orders, the fringe pattern is very close to a sinusoid and thus is well sampled with few pixels. Typically, we use 4x4 CCD pixels to sample a 2D MHM fringe, whereas a focal spot created by a microlens requires 16x16 pixels. Then when compared to Shack-Hartmann systems, the QWLSI technology offers 16 times more measurement points when using the same CCD. Consequently, combined with the high dynamic range measurement, the MHM has a very high spatial resolution (up to 96x72 measurement points for the infrared sensor and 300x400 for the high resolution sensor in the visible domain) [6].

3. FTM AND OPTICAL ABERRATION CHARACTERIZATION

3.1 Measurement principle

Wave front sensing techniques can be used to characterize optical aberrations as well as Fizeau or a Twyman-Green interferometry. However, the dynamic range of classical interferometer set-ups is not large enough to thoroughly measure remaining aberrations larger than 20 waves in spherical aberration. Moreover, double-passing aperture stops with highly aberrated beams lead to marginal ray filtering when the beam comes back. Therefore a measurement for the complete lens group aperture is not possible in this configuration. This is a major problem since it is well known that most aberrations occur at the edges. Therefore only direct wave front measurement is possible.

Thanks to the high dynamic range of QWLSI, Phasics proposes a set-up for direct wave front measurement. In this configuration, the characterization of lenses is very simple and easy to align: a calibrated collimated beam propagates through the lens, the transmitted wave front is then analyzed by the QWLSI wave front sensor (see Figure 4 for the

infinite/finite configuration, for finite/finite analysis, the collimated beam is simply replaced by a point source). If the lens is perfect, the measured wave front is spherical, if not, the distance to a sphere is then the lens aberrations. From the intensity and wave front maps, we can then calculate the Point Spread Function (PSF) and deduce the Modulation Transfer Function (MTF) of the lens.

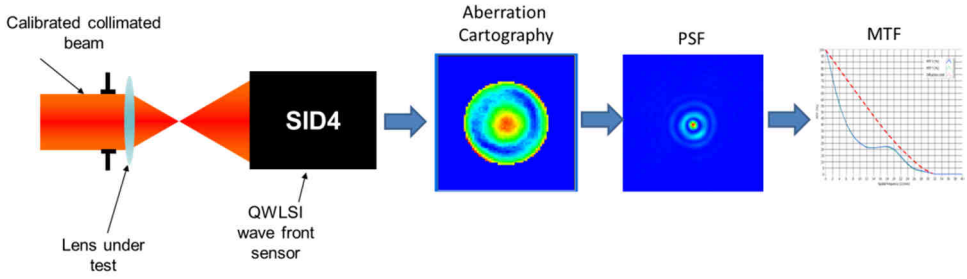

Figure 4 Principle of lens metrology with a QWLSI (here in infinite/finite configuration).

In this configuration, the wave front we measure is constituted of the divergence term (defocus, depending on the beam numerical aperture) and the deviation from a sphere term (aberrations). Knowing the wave front and the intensity cartographies, we are able to predict the PSF and thus the MTF in each propagation plane. This ability is very useful when evaluating MTF because we can exactly choose the observation plane (paraxial, best focus, …). More precisely, with through focus calculation, it is possible de determine the position in which the contrast at a given frequency is maximized and then calculate the MTF in this particular plane. The possibility to adapt the observation plane is equivalent to finding the focus plane in a classical MTF bench (see a concrete application of this ability in the following paragraph).

3.2 Experimental comparison

To validate our MTF measurement process, we compared our results and those obtained with a classical MTF bench. The comparison was achieved in the visible domain at λ=546nm. The lens under test has a focal length equal to 15,60mm and we studied this lens through a 3mm diameter diaphragm. The theoretical cut-off frequency is then equal to 352lp/mm. In the particular case described here, we wanted to obtain the MTF curve in the plane $P_{100lp/mm}$ where the contrast of the frequence 100lp/mm is maximized.

Measurement with QWLSI

The bench using a QWLSI sensor is described in paragraph 3.1. From the wave front measurement, we first have to find the plane $P_{100lp/mm}$. For that, we calculated the through focus MTF curve at 100lp/mm (see Figure 5, the curve is given in function of optical power in diopters). From that, we determine the position optimizing the contrast for this spatial frequency (here at 64,6 Diopters). We can then calculate the MTF in this particular plane (see Figure 7).

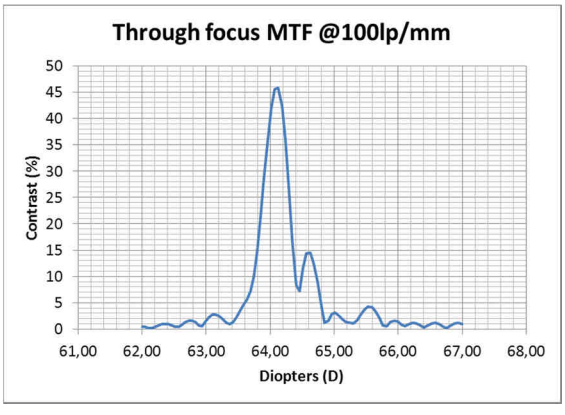

Figure 5 Through focus MTF at 100lp/mm

Classical MTF bench

The experimental MTF bench is described on Figure 6. It is based on measurement of contrast of MTF targets having different spatial frequencies according to the norm ISO 11979-2.

The bench uses a spatially incoherent source using a LED, a condenser and a diffuser. This source illuminates the MTF targets. The collimating lens f_L then creates the image of the MTF target at infinity, the lens is then studied in infinite/finite conjugate. The lens under test is placed afterwards and creates an image at a finite distance (at "image plane") of the target. This one is finally recorded through a magnification system (x10, NA=0.25) and a CCD camera. This optical system has been designed in order to have the smallest possible impact on the contrast measurement.

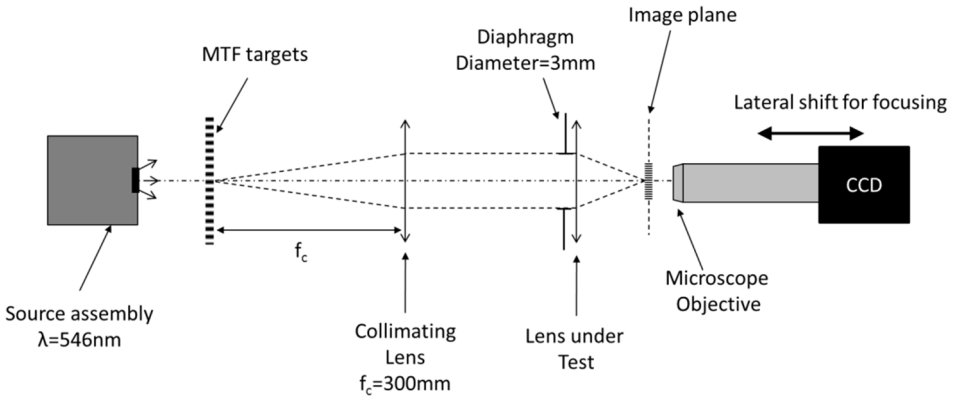

Figure 6 Scheme of the experimental MTF test bench

The image plane was adjusted in order to have the best possible contrast at 100lp/mm in the image side. After having found this position, we fixed the assembly microscope objective/CCD camera and studied 8 MTF targets to study the contrast from 14lp/mm to 250lp/mm (see results on Figure 7).

Comparison

The experimental results are displayed on Figure 7. It shows the results obtained with the direct analysis by QWLSI (continuous curve) and those obtained with the MTF bench (points). We also plotted the diffraction limited curve. The comparison shows a very good agreement between the two benches with a quadratic error lower than 5%.

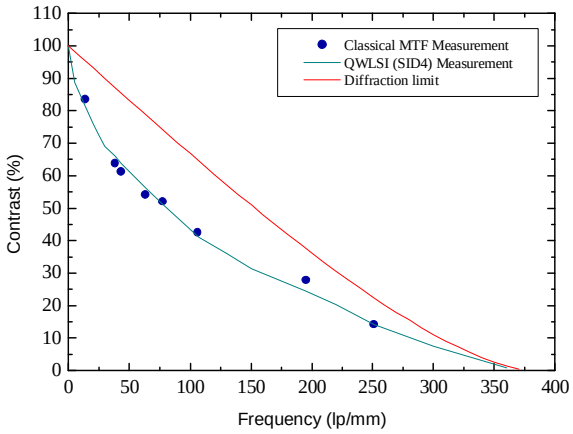

Figure 7 Experimental comparison of MTF measurement with QWLSI (continuous line) and with a classical MTF bench (points).

This study shows the ability to measure MTF with a high reliability. Compared to classical MTF benches, the measurement using a QWLSI is very fast (≈1s) as we measure the contrast for each frequency in one shot. Besides that, MTF by wave front sensing offers a great flexibility thanks to post-processing analysis (plotting profile in any direction or adapting the observation plane). The wave front measurement bench is also very easy to align compared to a classical

MTF bench. The lens under test has to be aligned with respect to the optical axis, and the wave front sensor is simply placed in the divergent beam; its position is just adapted to the beam size by a translation according the propagation axis. There is also no optical relay to align between the focal spot and the sensor.

4. APPLICATION TO MWIR AND LWIR LENS CHARACTERIZATION

4.1 DWIR wave front sensor

To develop our interferometer for MWIR and LWIR measurement, we first realized a MHM dedicated to the infrared region. We then chose a microbolometer array to record the interference pattern created by the MHM. Thanks to the use of a ULIS broadband microbolometer (see [7] and [8]) which is sensitive to wavelengths from 2 to 16µm, we obtained a single instrument for the MWIR and LWIR region. Based on this detector, the wave front sensor has a high spatial resolution (≈7000 measurement points). Besides the advantage of a broadband response, this uncooled technology makes the device easy to use and to integrate to a metrological measurement bench. The finalized instrument is called SID4-DWIR, for Dual Wavelength Infrared (see Figure 8).

Figure 8 SID4-DWIR, wave front sensor for wavelengths within 2 and 16µm

4.2 Application to analysis of a ZnSe lens in the MWIR and LWIR

We present here the analysis of a single ZnSe lens at two different wavelengths: λ_1=3.39µm (with an infrared HeNe laser) then at λ_2=10.6µm (with a CO_2 laser) using the SID4-DWIR. The bench is described on Figure 9.

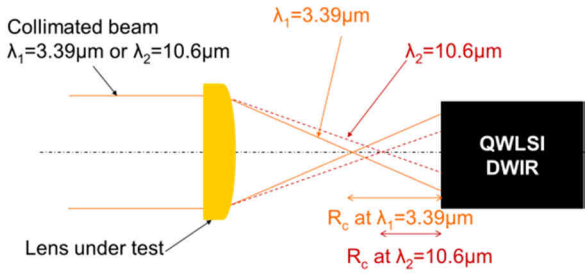

Figure 9 Scheme of the analysis of a ZnSe lens with a QWLSI at λ1=3.39µm and λ2=10.6µm

The specifications of the lens under test are: diameter=25.4mm, radius of curvature = 33.26mm ±1%. The lens was analyzed through a 8mm diameter diaphragm. The wave front sensor is placed at few millimeters after the focal spot. For both wavelengths, the wave front sensor was kept at the same position in order to study the displacement of the focal spot due to dispersion on the refractive index of the ZnSe.

The Table 1 shows the experimental analysis of the distance between the best focus position and the wave front sensor (i.e. the radius of curvature Rc of the divergent beam, see Figure 9). The comparison between the experimental displacement and the theoretical one shows a good agreement (error <2%).

	Experimental radius of curvature (best focus to wave front sensor)
λ_1=3.39µm	R_{C1}=23,340mm
λ_2=10.6µm	R_{C2}=22,780mm
Experimental Difference	R_{C2}- R_{C1}=-560µm
Theoretical Difference	ΔR_c^{theo}=-569µm

Table 1 Experimental analysis of the best focus position

On Figure 10, we show the wave front cartographies (the best sphere has been removed) and the calculated MTF and diffraction limit at both wavelengths. The experimental MTF at 3.39µm is highly deteriorated compared to the theoretical one. This is directly linked to the high spherical aberration generated by a plano-convex lens, particularly when the beam is incident on the flat face of the lens. At 10.6µm, the impact of the aberration is lower due to the higher wavelength, that is why the measured curve is close to the diffraction limit.

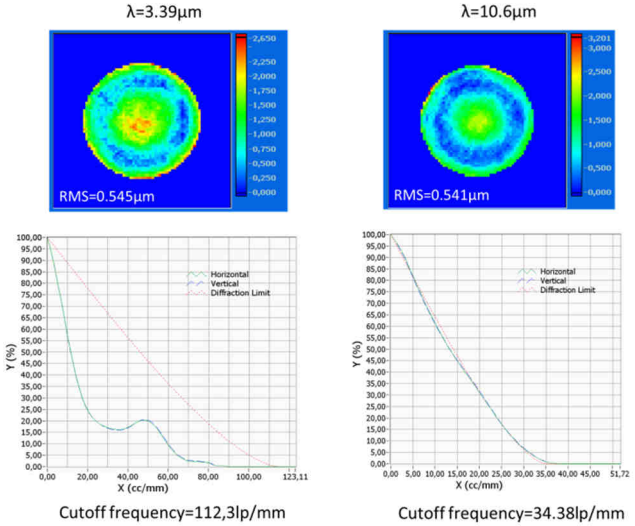

Figure 10 Experimental MTF curves at 3.39µm (left) and 10.6µm (right) obtained with the SID4-DWIR

We have also studied the spherical aberration term which is mainly present in the wave front cartography. The Table 2 gives the experimental and theoretical values.

	At λ_1=3.39µm	**At λ_2=10.6µm**	**Difference (λ_2 vs λ_1)**
F#	2.58	2.70	-
Exp. Zernike Spherical Ab. (RMS)	513nm	498nm	-15nm
Theoretical Zernike Spherical Ab.(RMS)	560nm	538nm	-22nm
Difference (Theory/Exp)	47nm (λ/72)	40nm (λ/265)	-

Table 2 Experimental analysis and comparison to theory

The comparison between experiment and theory shows in both cases a lower spherical aberration at 10.6µm with the same order of magnitude (-15nm for the experimental value and -22nmm for the theory) mainly due to a decrease of the numerical aperture of the beam. The study of the absolute value shows a slight difference, the experimental values are a little lower than those expected (47nm at 3.39µm and 40 nm at 10.6µm). At 10.6µm the impact of this difference is very low (the difference is of λ/265), but it can be significant at 3.39µm.

The incertitude on the radius of curvature (±1%) of the lens surface can explain this difference. Compared to the analysis with a classical MTF bench, which would have only shown a better MTF than expected (especially at 3.39µm), the analysis by QWLSI helps to give a diagnostic (here a supposed difference of the surface radius of curvature) of possible defects of the lens under test.

5. CONCLUSION

In this paper, we wanted to show the ability of Quadri-Wave Lateral Shearing Interferometry (QWLSI) to achieve qualification of optical systems in the infrared domain (MWIR and LWIR) with a high reliability and high flexibility. Our technique is a wave front sensor combining high dynamic range while keeping interferometric precision. Optical metrology by QWLSI gives, in one measurement, aberrations cartography and detail (defocus, spherical aberration, astigmatism, coma, …) but also the PSF and the MTF curves for any directions. To show the reliability of the MTF measurement by QWLSI we presented an experimental comparison of our results and those obtained through a classical MTF bench. This study showed a very good accordance between both benches. We also presented our instrument, the SID4-DWIR, for wave front sensing in both MWIR and LWIR wavelength ranges. Thanks to an analysis of a plano-convex ZnSe lens, we also pointed out another useful feature of QWLSI, the possibility to have a diagnostic of possible defects of the optical system under test.

Compared to classical MTF benches, the QWLSI technology offers a fast and easy to align solution to achieve a complete MTF analysis. Indeed, the alignment is very fast because no optical relay is required between the focal spot and the wave front sensor and the technique does not require to find the focusing plane. Moreover, with a single wave front analysis, we have access to an entire MTF evaluation: plotting MTF profiles for any direction, high precision contrast knowledge for each spatial frequency and possibility to adapt the observation plane.

ACKNOWLEDGMENTS

The authors are grateful to CIO and ERIO Teams from Onera for their support and their interest of this work.

REFERENCES

[1] Primot, J. and Guérineau, N. , "Extended Hartmann Test Based on the Pseudoguiding Property of a Hartmann Mask Completed by a Phase Chessboard," Appl. Opt. 39, 5715-5720 (2000).

[2] Shack, R. V. and Platt, B. C., "Production and use of a lenticular Hartmann screen," J. Opt. Soc. Am. 61, 656-660 (1971).

[3] Bon, P., Maucort, G., Wattellier, B. and Monneret, S., "Quadriwave lateral shearing interferometry for quantitative phase microscopy of living cells," Opt. Express 17, 13080-13094 (2009).

[4] Montgomery, W., "Self-Imaging Objects of Infinite Aperture," J. Opt. Soc. Am. 57, 772-775 (1967).

[5] Cohen-Sabban, Y. and Joyeux, D., "Aberration-free nonparaxial self-imaging," J. Opt. Soc. Am. 73, 707-719 (1983).

[6] Wattellier, B., Boucher, W. , Velghe, S., Francou, P., "High dynamic wave front sensing for lens group characterization," Proc. SPIE, Optifab (2011).

[7] Oelrich, B., Crastes, A., Underwood, C. and Mackin, S., "Low-cost mid-wave IR microsatellite imager concept based on uncooled technology," Proc. SPIE 5570, 209-217 (2004).

[8] Fieque, B., Crastes, A., Legras, O. and Tissot, J.-L. "MWIR uncooled microbolometer: a way to increase the number of applications," Proc. SPIE 5783, 531-538 (2005).